Journal of proteome research

pubs.acs.org/jpr

Article

Analysis of the Association between Fatigue and the Plasma Lipidomic Profile of Inflammatory Bowel Disease Patients

Diana Horta, Marta Moreno-Torres, María José Ramírez-Lázaro, Sergio Lario, Julia Kuligowski, Juan Daniel Sanjuan-Herráez, Guillermo Quintas,* Albert Villoria, and Xavier Calvet*

Cite This: *J. Proteome Res.* 2021, 20, 381−392

Read Online

ACCESS | Metrics & More | Article Recommendations

ABSTRACT: Inflammatory bowel disease (IBD) is a chronic, relapsing noninfectious inflammatory condition of the intestinal tract with two main phenotypes, ulcerative colitis (UC) and Crohn's disease (CD), and globally increasing incidence and prevalence. Nearly 80% of the IBD patients with active disease and 50% of those with inactive disease suffer fatigue with significant impairment of their quality of life. Fatigue has been associated with multiple factors in IBD patients but, in most cases, no direct cause can be identified, and risk factors in clinically quiescent IBD are contradictory. Furthermore, as the assessment of fatigue is subjective, there is an unmet clinical need for fatigue biomarkers. In this explorative study, we analyzed the plasma lipidomic profiles of 47 quiescent UC and CD patients (23 fatigued, 24 nonfatigued) using ultraperformance liquid chromatography−time-of-flight mass spectrometry (UPLC−TOFMS). The results showed changes in lipids associated with fatigue and IBD. Significantly decreased levels of phosphatidylcholines, plasmanyls, sphingomyelins, lysophosphatidylcholines, phosphatidylethanolamines, phosphatidylinositols, phosphatidylserines, and eicosanoids were observed in patients with fatigue. Network and metabolic pathway analysis indicated a dysregulation of the arachidonic acid and glycerophospholipid metabolisms and the sphingolipid pathway. The protein−metabolite interaction network showed interactions between functionally related metabolites and proteins, displaying 40 disease-associated hidden proteins including ABDH4, GLTP, and LCAT.

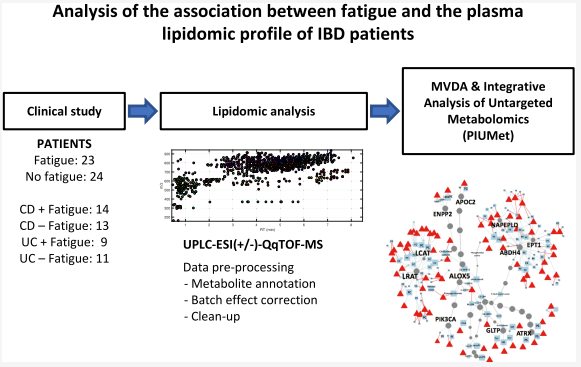

KEYWORDS: *inflammatory bowel disease, Crohn's disease, ulcerative colitis, fatigue, lipidomics*

INTRODUCTION

Inflammatory bowel disease (IBD) is a chronic, relapsing noninfectious inflammatory condition of the intestinal tract with two main phenotypes: ulcerative colitis (UC) and Crohn's disease (CD). Recent systematic reviews showed that incidence and prevalence of IBD have been globally increasing. In 2017, there were 6.8 million (95% UI 6.4.7.3) cases of IBD,[1] with the highest incidence (0.3%) in Western countries and rising incidence in newly industrialized countries,[2] showing the need for research on prevention and innovations in health-care systems to manage this disease. Although the pathogenesis of IBD is unknown, it has been suggested to be a multifactorial result of dysregulated immune responses, epithelial barrier defects, genetic predisposition, and environmental factors.[3,4]

Fatigue, defined as the "difficulty or inability to initiate or maintain activity", is highly prevalent in patients with IBD. Nearly 80% of the IBD patients with active disease and 50% of those with inactive IBD suffer fatigue with significant impairment of their quality of life.[5] The pathophysiologic mechanisms of fatigue in IBD patients have been associated with multiple factors, including sedentary lifestyle, active inflammation, anemia, nutritional deficiencies, physiological comorbidities, sleep disturbances, and altered microbiota and metabolism.[5] However, in most cases, no direct cause can be identified.[6] Although levels of fatigue are strongly associated with disease activity,[7] results found aiming at the association of fatigue with a proinflammatory state in clinically quiescent IBD are contradictory, at least partially, due to the subjective assessment of fatigue. Thus, the identification of objective fatigue biomarkers is of clinical and social significance. In this respect, metabolic profiling holds promise as a noninvasive tool in diagnosing and monitoring IBD. Various studies have shown significant alterations in lipid metabolism in UC and CD, and lipid metabolism and signaling have been suggested to play

Received: June 24, 2020
Published: September 24, 2020

https://dx.doi.org/10.1021/acs.jproteome.0c00462
J. Proteome Res. 2021, 20, 381−392

important roles in inflammation with significant implications for IBD and the use of lipidomic profiling of patients' plasma for IBD diagnosis.[8,9] However, to the best of our knowledge, the association of fatigue with changes in the plasma lipidome in UC and CD has not yet been investigated.

In this exploratory study, we analyzed the plasma lipidomic profile of 47 quiescent UC and CD patients (23 fatigued, 24 nonfatigued) for the identification of a metabolic phenotype associated with fatigue. Using ultraperformance liquid chromatography−time-of-flight mass spectrometry (UPLC−TOFMS) results obtained by unsupervised and supervised analysis showed a statistically significant difference between the lipid profiles associated with fatigue in IBD.

EXPERIMENTAL PROCEDURES

Ethical Considerations

The study was approved by the Ethics Committee of the Corporació Sanitària Parc Taulí (Institut Universitari Parc Taulí, Sabadell, Spain) and all methods were performed in accordance with relevant guidelines and regulations. Written informed consent was obtained from IBD patients prior to sample collection and analysis of demographics and clinical information.

Study Participants

The lipidomic analysis was carried out in the context of a larger study at the Hospital de Sabadell Gastroenterology Day Hospital (Sabadell, Spain) aiming at the analysis of the association of biological and psychological factors with IBD-related fatigue.[10] Patients completed a fatigue evaluation, which resulted in a fatigue score (FS) and psychological, quality of life, and IBD activity scores. Biological parameters were assessed, including levels of interleukins (IL-5, IL-8, and IL-12). Clinical activities of the diseases were assessed using the Harvey−Bradshaw score[11] for CD and the modified Mayo score for UC.[12] Five milliliters of peripheral blood samples were collected from UC and CD patients by venipuncture into EDTA-K3 tubes. Plasma was separated by centrifugation and frozen at −20 °C until further use.

Fatigue Questionnaire (FACIT-FS Score)

Fatigue was assessed using the Functional Assessment of Chronic Illness Therapy questionnaire. It comprises 40 items divided into five subscales: physical well-being, social/family well-being, emotional well-being, functional well-being, and fatigue subscale (FACIT-FS). FACIT-FS compiles 13 questions with five possible answers, from 0 (very fatigued) to 4 (not fatigued at all). The score of each subscale is the sum of the coded values of its items. The scores range from 0 to 52, with lower scores representing greater fatigue.[13]

Reagents and Materials

Liquid chromatography−mass spectrometry (LC−MS) grade acetonitrile (CH_3CN), isopropanol (IPA), and methanol (CH_3OH) were obtained from Scharlau (Barcelona, Spain) and formic acid (≥95%) and ammonium acetate (≥98%) from Sigma-Aldrich Quimica SL (Madrid, Spain). Ultrapure water was generated employing a Milli-Q Integral water purification system from Merck Millipore (Darmstadt, Germany).

Sample Preparation

Plasma samples were allowed to thaw on ice. Briefly, 150 μL of cold CH_3OH was added to 50 μL of plasma for protein precipitation. The mixture was homogenized (Vortex, 20 s) and centrifuged at 13 000*g* and 15 °C for 15 min. Further, 150 μL of the supernatant was evaporated to dryness (SpeedVac) and dissolved in 60 μL of (1:1) (5:1:4 IPA/CH_3OH/H_2O, 5 mM CH_3COONH_4, 0.1% v/v HCOOH)/(99:1 IPA/H_2O, 5 mM CH_3COONH_4, 0.1% v/v HCOOH). A blank extract was prepared following the same procedure but replacing plasma with water. For quality control, 10 μL of each sample extract was pooled in a glass vial to create a QC sample.

Lipidomic Analysis

The untargeted lipidomic analysis was carried out employing a 1290 Infinity HPLC system from Agilent Technologies (CA) equipped with a UPLC BEH C18 column (50 × 2.1 mm, 1.7 μm) from Waters (Wexford, Ireland). The flow rate was set to 400 μL min^{-1} running a binary mobile phase gradient starting at 98% of mobile phase A (5:1:4 IPA/CH_3OH/H_2O, 5 mM CH_3COONH_4, 0.1% v/v HCOOH) for 0.5 min, followed by a linear gradient from 2 to 20% of mobile phase B (99:1 IPA/H_2O, 5 mM CH_3COONH_4, 0.1% v/v HCOOH) for 3.5 min and from 20 to 95% v/v of mobile phase B in 4 min. Further, 95% v/v of mobile phase B was maintained for 1 min, and a return to initial conditions was achieved in 0.25 min and was maintained for a total run time of 14 min. The column and autosampler were kept at 55 and 4 °C, respectively, and the injection volume was 2 μL. For MS detection, an Agilent 6550 Spectrometer iFunnel quadrupole time-of-flight (QTOF) MS system working in the ESI+ and ESI− modes was used. Full scan MS data in the range between 70 and 1500 m/z were acquired at a scan frequency of 5 Hz using the following parameters: gas *T*, 200 °C; drying gas, 14 L min^{-1}; nebulizer, 37 psi; sheath gas *T*, 350 °C; and sheath gas flow, 11 L min^{-1}. Mass reference standards were introduced into the source for automatic MS spectra recalibration during analysis via a reference sprayer valve using the 149.02332 (background contaminant), 121.050873 (purine), and 922.009798 (HP-0921) m/z in ESI+ and 119.036 (purine) and 980.0163 (HP-0921+AcOH) in ESI− as references. ESI+ and ESI− analysis were carried out in independent batches. Between each mode, the instrument was cleaned and calibrated according to the manufacturer's guidelines. Each sample batch included 55 plasma samples (23 fatigue, 24 nonfatigue, and 8 additional samples excluded due to clinical criteria) in a randomized order, 12 QCs (1 QC for every 6 samples, 2 at the beginning of the sequence and 2 after the injection of the last plasma sample), and 4 blanks (1 at the beginning and 3 at the end of the sequence). QCs were used to monitor the instrument performance; correct within-batch effects; and identify unreliable, background, and carry-over features as described elsewhere.[14−16] A set of 9 QCs were injected at the beginning of each batch for system conditioning and MS/MS data acquisition. MS/MS spectra were acquired using the auto MS/MS method with the following inclusion m/z precursor ranges: 70−200, 200−350, 350−500, 500−650, 650−800, 800−950, 950−1100, and 1100−1200 from 70 to 1200 using, in all replicates, a rate of 5 spectra/s in the extended dynamic range mode (2 GHz), collision energy set to 20 V, an automated selection of five precursor ions per cycle, and an exclusion window of 0.15 min after two consecutive selections of the same precursor.

Data Preprocessing

Peak table generation was carried out using XCMS software.[17] The *centWave* method was used for peak detection with the following parameters: mass accuracy, 20 ppm; peak width,

https://dx.doi.org/10.1021/acs.jproteome.0c00462
J. Proteome Res. 2021, 20, 381−392

(3,15); snthresh, 12; and prefilter, (5,3000). A minimum difference in m/z of 7.5 mDa was selected for overlapping peaks. Intensity weighted m/z values of each feature were calculated using the *wMean* function. Peak limits used for integration were found through descent on the Mexican hat filtered data. Grouping before and after RT correction was carried out using the *nearest* method and 9 s as *rtCheck* argument. Finally, missing data points were filled by reintegrating the raw data files in the regions of the missing peaks using the *fillPeaks* method. The CAMERA package[17] was used for the identification of pseudospectra based on peak shape analysis, isotopic information, and intensity correlation across samples.[18] Each data set was processed with the following CAMERA functions: *xsAnnotate*, *groupFWHM*, *findIsotopes*, *groupCorr*, and *findAdducts* using standard arguments. Identification and elimination of noninformative features were carried out for ESI+ and ESI− data sets independently.

Within-batch effect correction was carried out using the nonparametric QC-SVRC approach employing a Radial Basis Function kernel, as described elsewhere.[19,20] The selection of the tolerance threshold (ε), the penalty term applied to margin slack values (C), and the kernel width (γ) was carried out using a preselection of C and optimization of ε and γ using a grid search, leave-one-out cross-validation, and the RMSECV as target function. C was selected for each LC−MS feature as the median value of the intensities observed in QC replicates. The ε search range was selected based on the expected instrumental precision (4−10% of the median value of the intensities observed for the whole set of QC replicates). The γ search interval selected was $[1, 10^6]$. Variables with more than 2 missing values in QC replicates, those with RSD(QC) > 20% after QC-SVRC, and for those for which the ratio between the median peak area values in QCs and blanks was lower than 6 were classified as unreliable and removed from further analysis.

Metabolite Annotation

Metabolite annotation (level ID: 2, putatively annotated compounds without matching to data for chemical standards acquired under the same experimental conditions) was carried out by matching experimentally acquired MS/MS spectra with the experimental HMDB, METLIN, and *in silico* LipidBlast[21] and MSDIAL MS/MS databases in accordance with the Metabolomics Standards Initiative (MSI) reporting standards,[22] as described elsewhere.[23] Briefly, the annotation algorithm determines whether each feature can be (pre)-annotated (m/z accuracy error <20 ppm) as the $[M + H]^+$, $[M + Na]^+$, $[M + NH_4]^+$, $[M + H + Na]^{+2}$, $[M + K]^+$, $[M + H + K]^{+2}$, $[M + H + CH_3CN]^+$, $[M + H + 2CH_3CN]^+$, $[M + Na + CH_3CN]^+$, $[M + 2Na\text{-}H]^+$, $[2M + H]^+$, $[2M + Na]^+$, $[2M + K]^+$, $[2M + NH_4]^+$, $[2M + H + CH_3CN]^+$, $[2M + Na + CH_3CN]^+$, or $[M + H\text{-}H_2O]^+$ adduct of, at least, one metabolite included in the MS/MS databases. In ESI−, the list of potential adducts included $[M\text{-}H]^-$, $[M + Cl]^-$, $[M + H_2O\text{-}H]^-$, $[M + 2Na\text{-}H]^-$, $[M + K\text{-}H]^-$, $[M + HAc\text{-}H]^-$, $[2M\text{-}H]^-$, $[2M + FA\text{-}H]^-$, $[2M + HAc\text{-}H]^-$, $[M + FA\text{-}H]^-$, and $[M + HAc\text{-}H]^-$. Then, if the feature was selected as a precursor within RT and m/z tolerances (0.1 min and 10 ppm, respectively), the closest experimental MS^2 spectrum is matched against the spectra of the potential metabolites included in the database. For each match, a spectral dot product (dp) and a reverse dot product (rdp) are calculated as described elsewhere.[24] The calculation of the rdp only included ions present in both the experimental and reference spectra. Then, the geometric mean of the *dp* and rdp is calculated, and the identity of the metabolite with the largest mean dot product is stored. Further parameters for metabolite annotation include: m/z accuracy in both precursor and fragment ions (10 ppm), the weight of m/z and intensity for the calculation of the dp and rdp[19] (in this study, m = 1.2 and n = 0.9 for dp and rdp, respectively), the minimum number of matching ions in the experimental and reference spectra (in this study, 4) detected above user-selected absolute and relative intensity thresholds (0.01% of the base peak and 500 AU, respectively), and a minimum mean dp (0.7, in this study). Also, to reduce the effect of co-fragmented features in the score, the intensities of peaks present in the experimental but not in the reference MS^2 spectrum were multiplied by 0.5.[20] When an LC−MS feature was annotated, features included in the same CAMERA *pcgroup*, also detected in the experimental and reference MS^2 spectra (with m/z accuracy error <10 ppm and intensity above an absolute and/or relative threshold), were labeled as fragments of the annotated metabolite. Metabolite annotation using LipidBlast was carried out using LipiDex as described elsewhere[19] using 0.01 Da tolerances in both MS (precursor) and MS^2 (fragment) data and the "LipidBlast Acetate" library.

Statistical Analysis

Multivariate principal component analysis (PCA) was carried out using autoscaling as data preprocessing. ANOVA simultaneous component analysis (ASCA) was used to quantify the amount of variation related to the type of disease (i.e., UC/CD), fatigue (yes/no), and their interaction, also using autoscaling as data preprocessing. Partial least squares were used for the development of multivariate discriminant models. Double cross-validation (2CV) was used for the assessment of the differences between groups (e.g., fatigue vs non-fatigue).[25] In 2CV, a randomly selected subset of samples was set aside by k-fold cross-validation (k-fold CV, k = 9 in this study) and used as a validation set. The remaining samples were then again split into train and test subset by leave-one-out-fold CV for the optimization of the PLS-DA classifier used to predict the test samples. The procedure was repeated until all samples were included once in the validation set and, then, an estimate of the discrimination between classes was calculated using the set of predictions. This way, samples used for the evaluation of the model performance were excluded from model development. The procedure was repeated a number of times (9 in this study) to average the effect of the initial random k-fold CV on the results. The statistical significance of 2CV PLS-DA figures of merit (e.g., classification accuracy, AUROC) was estimated by permutation testing as described elsewhere,[26] using a p-value < 0.05 as the threshold. The Prize-collecting Steiner forest algorithm for the integrative analysis of untargeted metabolomics (PIUMet) algorithm[27] was used for pathway analysis using the following parameters: prize function, −log (p-value); number of trees, 10; edge reliability, 2; negative prize degree, 0.0005; and number of repeats, 3. Comparison of proportions (e.g., the ratio of females in the fatigue and nonfatigue groups) was carried out using the "$N-1$" chi-squared test. The t-test was used to test the null hypothesis that the continuous data in two groups (e.g., fatigue vs non-fatigue) comes from independent random samples with equal means and unknown variances,

https://dx.doi.org/10.1021/acs.jproteome.0c00462
J. Proteome Res. 2021, 20, 381−392

Table 1. Clinical and Demographic Data of the Patients Included in the Study

	UC/CD		CD		UC	
	F	NoF	F	NoF	F	NoF
sample size	23	24	14	13	9	11
fatigue score (mean ± SD)	23 ± 6	46 ± 7	22 ± 6	44 ± 9	24 ± 5	48 ± 3
sex (male/female)	9/14	11/13	6/8	6/7	3/6	5/6
age (years) (mean ± SD)	37 ± 12	38 ± 10	37 ± 12	34 ± 8	37 ± 14	42 ± 11
illness duration (years) (mean, median, range)	9, 6, 1−40	9, 6, 2−18	8, 7, 2−19	8, 7, 3−15	10, 5, 1−40	9, 8, 2−18
smoker (yes/no)	9/14	10/14	6/8	7/6	3/6	3/8
IL-12 (p70) (pg mL^{-1}) (mean ± SD)	7 ± 18	0.5 ± 1.5	3.4 ± 6.1	0	12.7 ± 29.3	1.1 ± 0.6
IL-5 (pg mL^{-1}) (mean ± SD)	0.91 ± 1.82	0.9 ± 3.7	1.2 ± 2.2	1.5 ± 5.3	0.4 ± 0.7	0.3 ± 0.1
IL-8 (pg mL^{-1}) (mean ± SD)	1 ± 2	1.74 ± 2.61	0.5 ± 1.0	1.9 ± 3.2	2.0 ± 2.1	1.7 ± 2.0
body mass index (mean ± SD)	25 ± 5	25 ± 5	26 ± 6	26 ± 6	24 ± 3	24 ± 3
fatigue score (mean ± SD)	23 ± 6	46 ± 7	22 ± 6	44 ± 9	24 ± 5	48 ± 3

without assuming that the populations also have equal variances.

Software

Data acquisition and manual integration were carried out employing MassHunter Workstation (version B.07.00) from Agilent. Raw data (.D) was converted into mzXML format using ProteoWizard (http://proteowizard.sourceforge.net/). Peak detection, integration, deconvolution, alignment, and pseudospectra identification were carried out using XCMS and CAMERA in R 3.6.1. Metabolite annotation and data analysis were carried out in MATLAB 2017b (Mathworks Inc., Natick, MA) using in-house written scripts and the PLS Toolbox 8.7 (Eigenvector Research Inc., Wenatchee). MATLAB functions for QC-SVRC, annotation, and data cleanup used in this work are available with the authors. Network analysis was carried out using PIUMet[27] (http://fraenkel-nsf.csbi.mit.edu/piumet2/). Pathway analysis was carried out with MetaboAnalyst 4.0.[28] Metadata, raw LC−MS, and LC−MS/MS data (as.mzxml and. ms2 files); the peak tables generated using XCMS-CAMERA (as.csv files); the curated and annotated peak table (as.mat files); MATLAB scripts used for data processing; and the network of protein−protein and protein−metabolite interactions inferred by PIUMet (as. html file) are available at the Zenodo repository (zenodo.org/deposit/3906482).

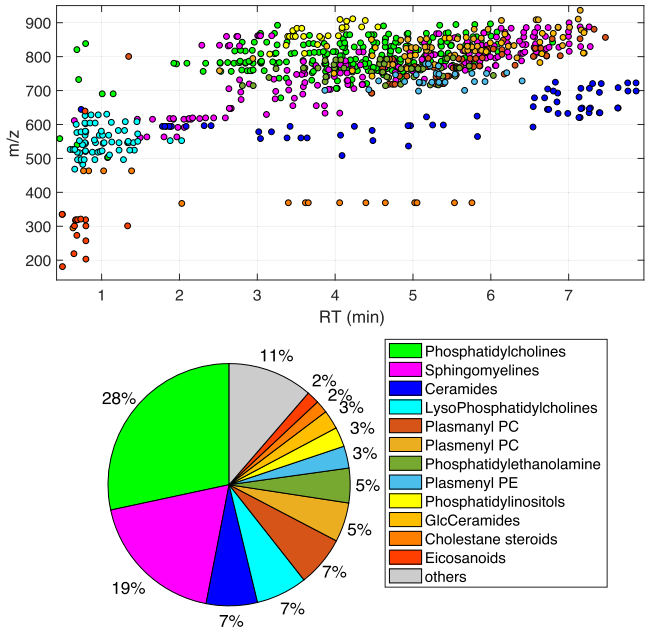

Figure 1. (Top) Distribution of LC−MS annotated features and classes retained after data preprocessing. (Bottom) Pie plot representing the relative percentages of annotated features of each subclass with respect to the whole data.

RESULTS

Overview of the Lipidomic Profiles

Clinical and demographic data are summarized in Table 1. A previous study showed that fatigue was significantly related to gender, Crohn's disease, and body mass index.[29] No statistically significant differences (p-values > 0.05) between their distributions in fatigued and nonfatigued patients were observed and so these variables were excluded as confounding factors in this study.

Figure 1 summarizes the main lipid subclasses of the features annotated in the ESI+ and ESI− data sets after data preprocessing and cleanup. The classes with the largest numbers of annotated lipids were glycerophosphocholines, sphingolipids (SLs), glycerophospholipids, and glycerophosphoethanolamines with phosphatidylcholines (PCs), sphingomyelins (SMs), ceramides, lysophosphatidylcholines (LysoPCs), plasmanyl and plasmenyl PCs, and phosphatidylethanolamines (PEs) accounting for 77% of the 952 annotated LC−MS features (483 and 469 measured by ESI+ and ESI−, respectively).

Principal component analysis (PCA) was used for an initial explorative analysis of trends in the data set. Figure 2 shows the score plots of a two-component PCA model explaining 35% of all variation. The random distribution of PC1 and PC2 scores of QC replicates as a function of the injection order and the tight clustering of the QCs in the PC1−PC2 score depicted in Figure 2 supported the instrumental stability throughout the analysis. PCA score plots showed a high overlap across the fatigue and nonfatigued patients independent of the type of IBD and also between IBD patients with and without fatigue, indicating that neither the type of disease nor the presence of fatigue was among the main sources of variance in the data.

ANOVA simultaneous component analysis (ASCA) was then used to quantify the amount of variation related to the type of disease (i.e., UC/CD), fatigue (yes/no), and their interaction on the metabolic profiles. ASCA provides a multivariate ANOVA by applying a simultaneous component analysis to each of the effects modeled by an ANOVA.[30] In this study, the ANOVA model included two-way interactions of two factors: $X = \text{mean} + X_{\text{disease}} + X_{\text{fatigue}} + X_{\text{disease−fatigue}} + E$.

https://dx.doi.org/10.1021/acs.jproteome.0c00462
J. Proteome Res. 2021, 20, 381−392

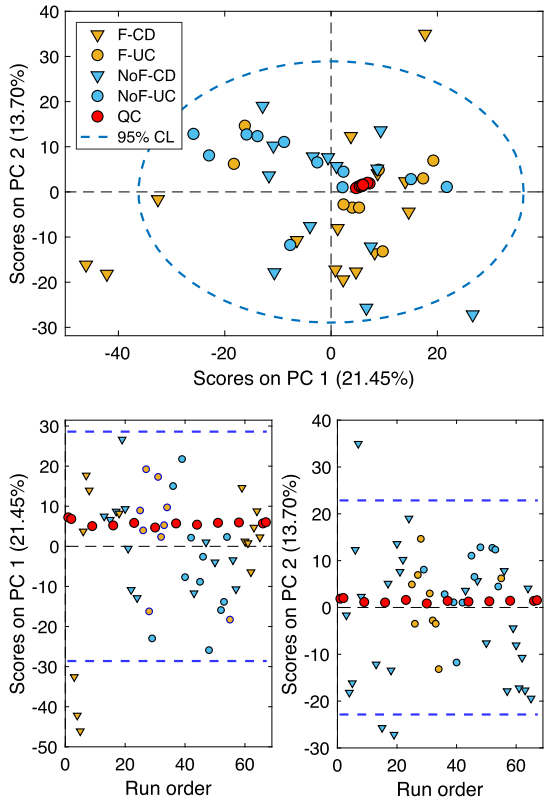

Figure 2. PCA score plots from the analysis of LC−MS data. (Top) PC1 vs PC2 scores. (Bottom) PC1 and PC2 scores as a function of the injection order.

The results summarized in Table 2 revealed that the dominant part of the variation was unrelated to the two considered factors or their interaction. However, results showed small contributions of fatigue (p-value = 0.05) and no effect for "disease" or the interaction between disease and fatigue. PC scores of the ASCA factor "fatigue" (i.e., $X_{fatigue}$) are depicted in Figure 3. In this model, the effect associated with fatigue, previously masked by other sources of variability (e.g., between-individual variation) in the initial PCA, could be observed. Likewise, Figure 3 shows a heatmap visualization of the clustering according to fatigue using, for better visualization, the top 50 most discriminant features in $X_{fatigue}$.

Table 2. Relative Contributions of the Effect of Fatigue, IBD (UC, CD), and Their Interaction to the Total Variation Estimated by ASCA

term	PC	effect	p-value[a]
mean		0.00	
disease	1	3.06	0.2
fatigue	1	3.33	0.05
disease × fatigue	3	2.32	0.3
residuals		91.45	

[a] p-Values were estimated using 1000 permutations.

Association of Fatigue and the Lipidomic Profile in IBD Patients

Supervised PLS-DA was carried out for the assessment of the class separation between fatigued and nonfatigued groups of IBD patients and for the identification of a metabolic phenotype associated with fatigue. A double cross-validation

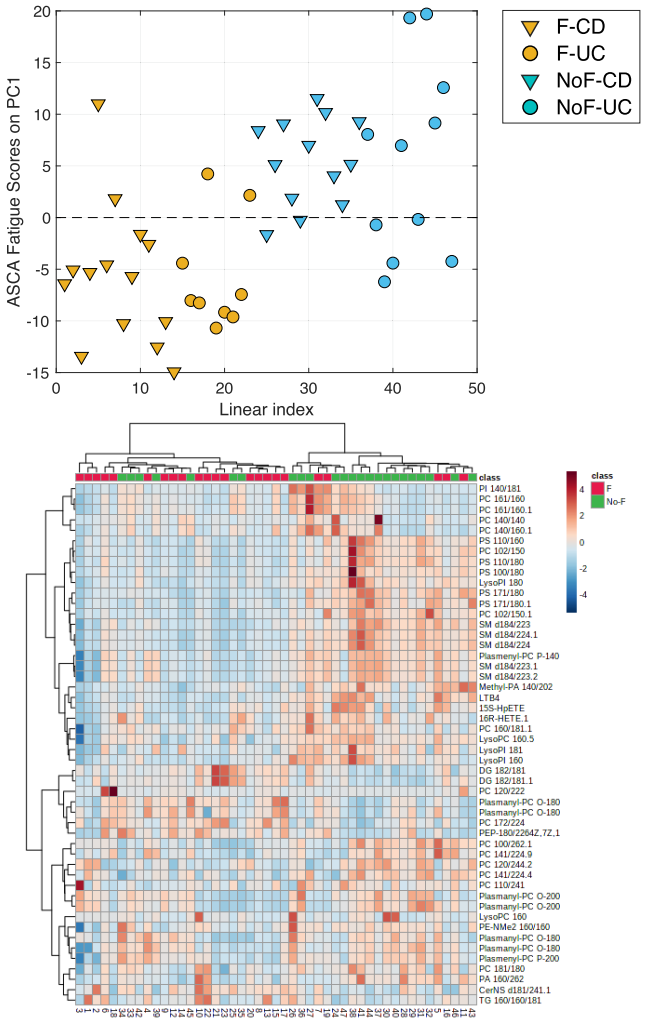

Figure 3. (Top) ASCA scores on PC1 of the factor fatigue ($X_{fatigue}$). (Bottom) Heatmap visualization based on the 50 most discriminant biomarkers in $X_{fatigue}$. Rows: LC−MS features; columns: samples. Green: fatigued patients; red: nonfatigued patients. Color key indicates the intensity of the LC−MS feature: blue: lowest; red: highest.

(2CV) strategy was selected for model development and for the assessment of its generalization accuracy.[25] Figure 4A shows the 2CV-PLSDA predicted values for the classification of samples collected from CD and UC patients (classification accuracy-CV = 67%, AUROC-CV = 0.68, see Table 3). The statistical significance (p-values < 0.05) of the discrimination of fatigued patients was performed by permutation testing using 250 permutations.[31] Figure 4B shows the histograms of the null reference distributions of the classification accuracy and AUROC estimates obtained using randomly assigned class labels and the mean values obtained using real class labels. The assessment of the class separation between fatigued and nonfatigued was then carried out separately for UC and CD patients, using leave-one-CV due to the limited sample sizes (20 UCs and 27 CDs). Results obtained indicated a better discrimination of fatigue in CD patients (classification accuracy-CV = 74%, AUROC-CV = 0.80, permutation test p-values < 0.05) than in UC patients (classification accuracy-CV = 67%, AUROC-CV = 0.62, permutation test p-values > 0.05). However, due to the limited sample sizes and the expected high interindividual variability, it is difficult to

https://dx.doi.org/10.1021/acs.jproteome.0c00462
J. Proteome Res. 2021, 20, 381−392

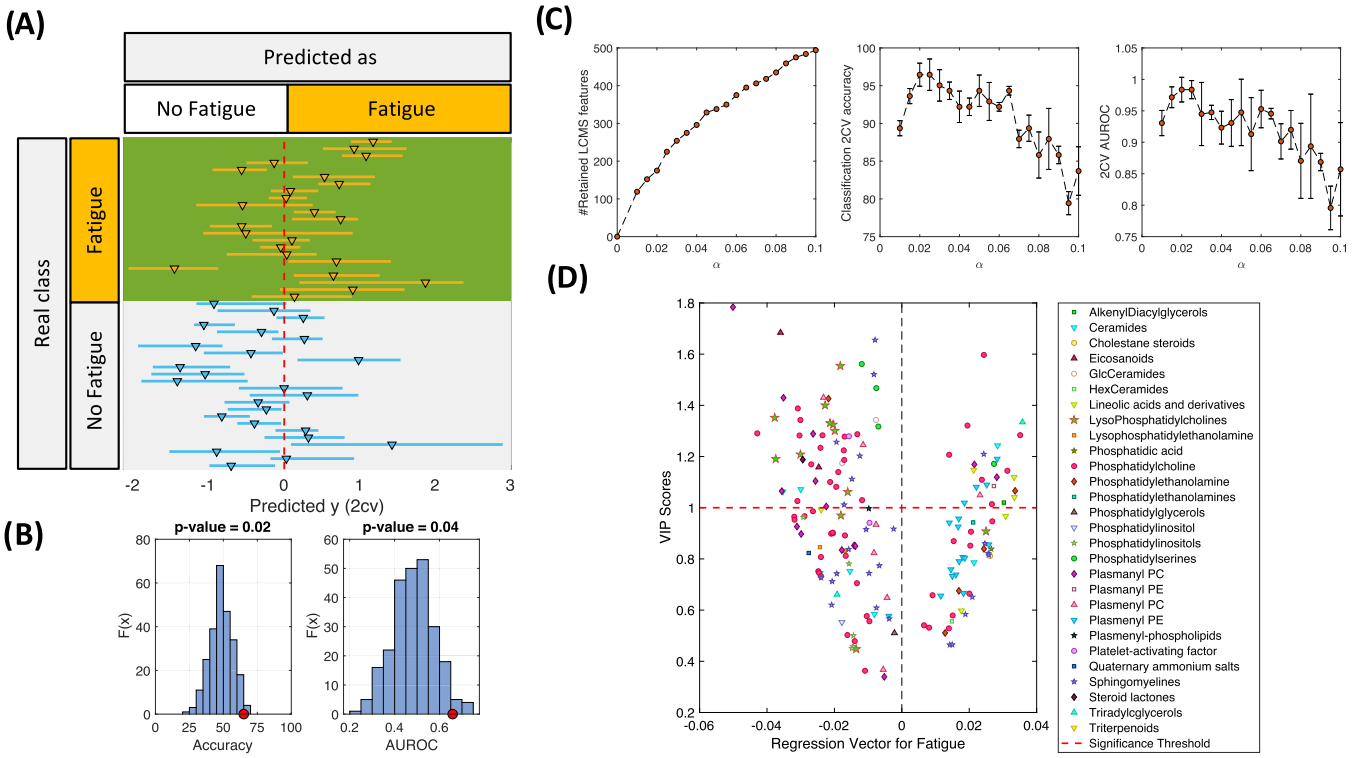

Figure 4. (A) Sample predicted values by PLS−DA for the discrimination between fatigue and nonfatigued patients. (B) Results from the permutation test for the assessment of the PLS−DA discrimination between fatigue and nonfatigued patients depicted in (A) using the classification accuracy and the AUROC as figures of merit. (C) Evolution of the number of retained features, CV-classification accuracy, and AUROC value as a function of the selected threshold for feature selection. (D) Value of the retained discriminant features in the PLS−DA regression vector after feature selection and their corresponding VIP scores.

Table 3. Confusion Table Calculated Using the Mean 2CV Predicted Classes

	predicted class	
real class	fatigue	no fatigue
fatigue	17	6
no fatigue	9	15

estimate the significance of this difference or to provide a biologically relevant interpretation of the results.

A combination of complementary univariate and multivariate methods[32] was used for the identification of metabolites associated with fatigue in IBD. The first strategy involved a data-driven feature selection in the PLS-DA models using the mean PLS-DA regression vector estimated from the set of PLS-DA models built using real class labels (b_{true}) and the set of 250 mean regression vectors from the set of PLS-DA models built using randomly permuted class labels as null distribution (b_{perm}).[33] A LC−MS feature was labeled as associated with fatigue if its value in the b_{true} vector did not belong to the distribution of the b_{perm} values of this considered metabolite. The confidence level was empirically selected by analyzing the evolution of the classification performance estimates as a function of the confidence level in a series of models built using stepwise backward elimination of features with p-values < threshold until no further features were excluded. A confidence level = 0.02 was selected based on results depicted in Figure 4C, enabling the selection of 205 LC−MS features including PCs, SMs, plasmenyl PEs, plasmanyl PCs, LysoPCs, and ceramides (see Table 4). Figure 4D shows the VIP scores and PLS-DA regression vector values of each feature in a model developed using the selected LC−MS features and three latent variables.

The second strategy for the identification of discriminant features involved univariate t-tests carried out to test the null hypothesis that the data of the fatigue and nonfatigue groups came from independent random samples with equal means with unknown and unequal variances. Results identified 111 (12% of the total of the annotated features) for which the t-test rejected the null hypothesis at the default 5% significance level (see Table 4). The two strategies identified a total of 251 unique LC−MS features that indicated that the largest differences in the lipidomic profiles of fatigued patients were associated with glycerophospholipids, sphingolipids, and fatty acyls. However, the sets of features selected as discriminants showed a limited overlap and only 65 of them were commonly selected as discriminants by t-test and PLS-DA, including glycerophosphocholines, glycerophospholipids, sphingolipids, and glycerophosphoethanolamines.

Pathway Analysis

To extract more information, the Prize-collecting Steiner forest algorithm for Integrative Analysis of Untargeted Metabolomics (PIUMet) algorithm[27] was used for the analysis of the set of 251 annotated features classified as discriminants by at least one of the abovementioned strategies. Figure 5 shows the network of protein−protein and protein−metabolite interactions inferred by PIUMet (the network including the metabolite peaks and names of the hidden proteins and metabolites is available as. html at the Zenodo repository (zenodo.org/deposit/3906482)). Further, 104 LC−MS features were matched to 165 metabolites in the PPMI network.

https://dx.doi.org/10.1021/acs.jproteome.0c00462
J. Proteome Res. 2021, 20, 381−392

Table 4. Subclasses of Annotated Features Selected as the Discriminant in the PLS-DA Model or by the *t*-Test[a]

subclass	PLS-DA (b+)	PLS-DA (b−)	*t*-test (N^+)	*t*-test (N^-)
phosphatidylcholine	17	35	7	24
plasmanyl PC	2	12	7	5
lysophosphatidylcholines	1	11	1	11
plasmenyl PE	16	1	4	0
phosphatidylserines	1	3	1	7
plasmenyl PC	1	6	2	3
phosphatidylethanolamine	4	1	0	0
phosphatidylinositols	0	5	0	0
lysophosphatidylethanolamine	0	2	0	1
phosphatidylinositol	0	1	0	1
phosphatidylglycerols	0	1	0	0
sphingomyelines	8	17	1	13
ceramides	2	5	1	0
GlcCeramides	0	2	0	2
ceramidesamide-1-phosphates	0	0	0	1
HexCeramides	1	0	0	0
eicosanoids	0	2	0	7
linoleic acids and derivatives	4	1	0	0
triradylcglycerols	1	1	1	0
diglycerides	0	0	2	0
alkenyldiacylglycerols	1	0	0	0
phosphatidylethanolamines	1	0	0	2
cholestane steroids	1	0	0	1
steroid lactones	0	1	0	1
plasmanyl PE	1	0	0	0
platelet-activating factor	0	2	0	1
lysophosphatidylinositol	0	0	0	3
triterpenoids	1	0	1	0
plasmenyl-phospholipids	0	1	0	0
phosphatidic acid	1	0	0	0
quaternary ammonium salts	0	1	0	0

[a]Features selected were split into those showing a statistically significant positive or negative association with fatigue according to the sign of its value in the PLS-DA regression vector (b^+ or b^-) or according to the ratio between the mean values in fatigue vs nonfatigue.

PIUMet identified a network that connected 104 LC−MS peaks (41%) through hidden proteins and metabolites. Pathway analysis using the metabolites included in the network indicated a dysregulation of the arachidonic acid (p-value < 0.003) and glycerophospholipid metabolisms (p-value < 0.05) and the sphingolipid pathway (p-value < 0.05). The protein−metabolite interaction network showed interactions between functionally related metabolites and proteins, displaying 42 disease-associated proteins (i.e., hidden proteins in the network), including ABHD4, GLTP, ATRX, EPT1, LCAT, LRAT, and ALOX5.

DISCUSSION

Fatigue is a complex sensation that is perceived as the loss of overall energy and a feeling of exhaustion. In the current study, we characterized the plasma lipidome of UC and CD patients who did or did not present fatigue. Results obtained revealed that plasma lipidomic profiles of IBD patients were significantly altered in patients with fatigue compared to patients without fatigue. Significantly decreased levels of PCs, SMs, LysoPCs, PEs, PIs, PSs, and eicosanoids were observed in patients with fatigue. Pathway analysis revealed alterations in arachidonic acid, glycerophospholipid, and sphingolipid metabolism, suggesting an association between lipid pathways and fatigue, which may influence the distinct symptomatology found in UC and CD patients.[34]

SLs are bioactive lipids that contribute to shaping membranes, to the arrangement of lipid rafts,[35,36] and to regulate diverse cellular functions including cell signaling, secretion, and endocytosis.[37,38] In inflammatory disease, there is a two-way interaction between SLs and oxidant production whose interplay regulates the outbreak and spread of oxidative stress. On the one hand, increased reactive oxygen species (ROS) levels, decreased antioxidant defenses, and activation of NO synthase or/and NADPH oxidase can promote the turnover of complex SLs into bioactive hydrolytic products like ceramides, sphingosine, and sphingosine-1 phosphate. On the other hand, some SLs may disrupt mitochondrial electron transport increasing ROS production.[39] Among the different SLs, sphingomyelin metabolism is interesting because ceramides, the direct hydrolytic products of SM, and sphingosine-1-P are important in immunity, inflammation, and inflammatory disorders.[40] The sphingomyelinase (SMase) family is a group of enzymes that hydrolyzes SM to ceramide and phosphocholine. It has been described as an increase in the sphingomyelinase activity in response to oxidative stress and inflammation. Given the effects of oxidant activity on the contractile function of skeletal muscle,[41,42] SL levels, by stimulating oxidant production, can influence muscle strength and promote fatigue.[43] This hypothesis is supported by recent data where direct exposure to recombinant SMase depressed the isometric force of intact-fiber bundles from the murine diaphragm, demonstrating that SMase/ceramide signaling promotes fatigue by stimulating oxidant production.[44] Our results evidence a significant decrease in the SM level in the fatigue group, suggesting that SMase activity could be increased in these patients, resulting in higher levels of ceramides and sphingosine-1-P products that may induce oxidative stress and fatigue. Although no general accumulation of ceramides is observed in these patients, Cer(d18:1/24:1) appeared to increase in the fatigue group. Ceramides can also be synthesized by other pathways, including the participation of certain microorganisms and cytokines.[45] For instance, lipopolysaccharide constituent of the outer membrane of Gram-negative bacteria activates acid SMase in macrophages.[45,46] Lecithin-cholesterol acyltransferase (LCAT) is a secretory protein primarily produced in the liver. It is a central enzyme in the extracellular metabolism of plasma lipoproteins responsible for the esterification of cholesterol on the surface of lipoproteins, particularly in high-density lipoproteins (HDLs), and the synthesis of most of the cholesteryl esters in human plasma. The plasma levels of HDL are positively correlated with this enzyme activity and therefore its regulation is of clinical interest.[47] LCAT is also a critical component of the pathway of reverse transport of cholesterol from peripheral tissues to the liver for excretion. SM is also a physiological inhibitor of LCAT.[47] Further quantitative analysis of ceramide and sphingomyelin concentrations and oxidative stress products needs to be performed to study these hypotheses.

In addition, the inferred protein−metabolite interaction network revealed GLTP as a fatigue-associated protein. GLTP catalyzes the intermembrane transfer of various glycosphingolipids. Currently, there is a debate whether *in vivo* GLTP functions as an intermembrane transporter of GSLs or as a sensor of SL metabolic homeostasis.[48−52] SL metabolic

https://dx.doi.org/10.1021/acs.jproteome.0c00462
J. Proteome Res. 2021, 20, 381−392

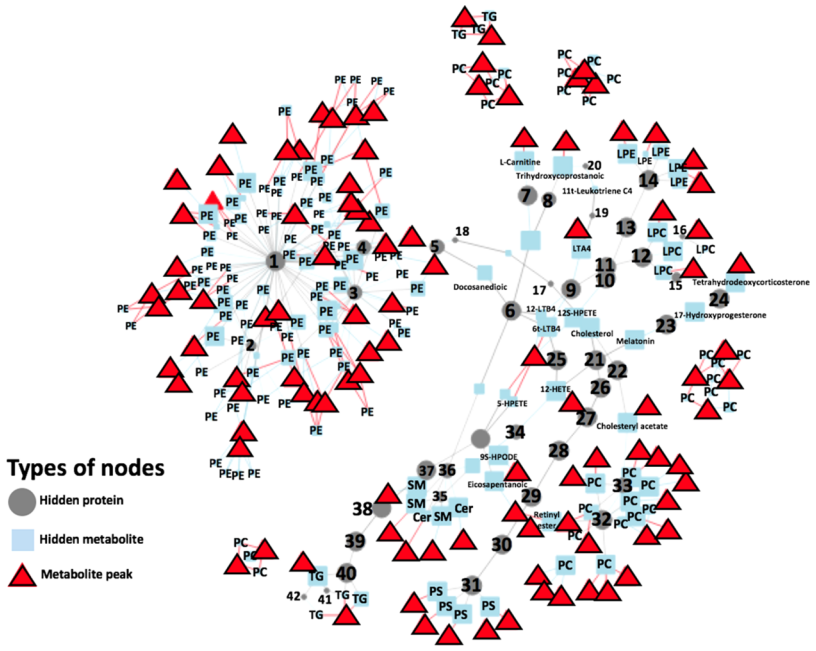

Figure 5. Network of protein−protein and protein−metabolite interactions inferred by PIUMet, using the subset of 180 features selected as discriminants (see the file available at the Zenodo repository (zenodo.org/deposit/3906482) for a detailed version of the network including the metabolite peaks and names of the hidden proteins and metabolites). Hidden proteins: 1, ABHD4; 2, EPT1; 3, NAPEPLD; 4, CSNK2B; 5, ADH5; 6, CYP4F2; 7, SLCO1B1; 8, ABCB11; 9, LTA4H; 10, ALOX12; 11, MCC; 12, PAFAH1B2; 13, ITGB4; 14, ENPP2; 15, PLA2G7; 16, PAFAH2; 17, ABCA1; 18, PISD; 19, LTC4S; 20, SLCO1B3; 21, POR; 22, SOAT1; 23, CYP1B1; 24, AKR1C1; 25, CYP4F12; 26, FANCC; 27, FANCE; 28, FANCD2; 29, BRCA2; 30, RAD51; 31, ATRX; 32, LRAT; 33, LCAT; 34, CYP4B1; 35, GM2A; 36, GLTP; 37, MAPKAP2; 38, HSPB1; 39, CRYAB; 40, APOC2; 41, PLIN4; and 42, AGPAT9.

labeling concurrent with GLTP overexpression has previously revealed alterations in *de novo* sphingolipid production, demonstrating a direct role of GLTP in the regulation of SL homeostasis. The observed changes included increased GlcCer synthesis and decreased sphingomyelin synthesis but no changes in GalCer or LacCer synthesis.[53] These results support that differential GLTP expression levels in the fatigued patients could contribute to altering the SL metabolism. Furthermore, recent proteomic studies in mice also evidenced a GLTP role in the neuronal myelination process.[54,55] Given the association of myelination degree in the nervous system with chronic fatigue syndrome,[56] and sphingolipids being critical myelin components, this gives rise to the possibility that IBD patients suffering fatigue may have altered GLTP expression with perturbed myelination events. To confirm these hypotheses, additional evaluation of the expression levels of GLTP enzyme is required, which could reveal individual variations among IBD patients linked to different susceptibilities to suffer from fatigue.

Glycerophospholipids are glycerol-based phospholipids. They are the main components of the cell membranes and act as binding sites for intracellular and intercellular proteins. They are also an important energy reservoir and are bioactive molecules in signal transduction processes.[57,58] Several chronic clinical conditions are characterized by membrane damage, mainly oxidative but also enzymatic, resulting in loss of cellular function. This is apparent in mitochondrial inner membranes, where oxidative damage to phospholipids results in loss of transmembrane potential, electron transport function, and generation of high-energy molecules. The phospholipids of mitochondria are especially sensitive to oxidative damage because of their high content of certain unsaturated fatty acids, such as docosahexaenoic acid (DHA) and eicosapentaenoic acid (EPA). Several studies have described altered glycerophospholipid levels in IBD patients and in chronic fatigue syndrome.[59] Interestingly, recent clinical trials have evidenced the benefits of lipid replacement therapy, which implies the use of oral supplements containing membrane phospholipids and antioxidants. They have demonstrated to restore mitochondrial function and reduce fatigue in patients with a wide variety of clinical diagnoses characterized by loss of mitochondrial function presenting fatigue as the main symptom.[60] This evidence supports the association found in this analysis between the downregulation of glycerophospholipids and fatigue.

Abnormal metabolism of arachidonic acid (AA) in IBD has been previously reported.[61] AA is a 20-carbon chain polyunsaturated fatty acid with four double bonds present in the phospholipids of biological cell membranes, conferring fluidity and flexibility.[62] Skeletal muscle is one of the main reservoirs of AA, accounting for approximately 10−20% of the phospholipid fatty acid content.[63] The four double bonds of AA predispose its interaction with proteins and to peroxidation, producing bioactive oxygenated molecules including eicosanoids and isoprostanes (IsoPs). IsoPs are a group of peroxidation products of AA produced by a noncyclooxigenase free-radical-catalyzed mechanism, mainly driven by ROS, which has been found elevated in the urine of IBD patients compared to healthy volunteers.[64] These molecules have overwhelming importance as cell signaling molecules with functions in the immune system.[65] Besides by direct consumption of dietary food or consumption of the parent molecule linoleic acid, endocannabinoids such as *N*-arachidonoyl ethanolamine (anandamine, AEA) serve as an endogenous source of AA.[66] AA mediates inflammation either directly or as previously mentioned, upon its conversion into

https://dx.doi.org/10.1021/acs.jproteome.0c00462
J. Proteome Res. 2021, 20, 381−392

eicosanoids. On a cellular level, AA and DHA deficiencies result in deleterious effects on cell membranes, which lose their normal flexibility and become more rigid, perturbing the protein receptor molecules and affecting cell signaling. Previous works also linked AA levels and chronic fatigue syndrome supported by lower levels of both DHA and AA in red blood cells of chronic fatigue syndrome patients, indicating a state of unbalanced oxidative stress.[67] In this study, lower levels of leukotriene B4, the major metabolite in neutrophil polymorphonuclear leukocytes, and a product of the 5-lipoxygenase pathway of AA metabolism were also observed in fatigue (FC = −0.52, *t*-test *p*-value < 0.05).

Although AA was not detected in our analysis, our results showed a downregulation of eicosanoid levels in patients with fatigue. In addition, the inferred protein−metabolite interaction network revealed ABHD4 as a disease-associated protein. ABHD4 is lysophospholipase selective for N-acyl phosphatidylethanolamine, contributing to the biosynthesis of *N*-acyl ethanolamines.[68] ABHD4 is involved in the metabolic synthesis, degradation, and oxidation pathway of the lipid mediator AEA, the endogenous precursor of AA.[69,70] These results suggest that a putatively altered expression of ABHD4 in IBD patients suffering from fatigue would affect AEA and consequently AA levels, leading to lower levels of eicosanoids. Disturbed ABHD4 expression and eicosanoid levels would be a source of susceptibility to suffer from fatigue in IBD patients. To evaluate this hypothesis, further targeted analysis of AA metabolism and the study of ABHD4 expression levels need to be performed.

This is a small exploratory study that provided preliminary results, which need to be validated in future studies with larger sample sizes. Although 2CV provided external figures of merit supporting a statistically significant difference between fatigue and nonfatigue patients, an external validation will provide a better estimation of the generalization performance than that provided by 2CV and it will support the identification of potential biases and confounding sources.

Besides, the comprehensive analysis of the plasma lipidome is extremely challenging due to a large number of metabolite classes with different concentrations and physicochemical properties. The employed LC−MS/MS data acquisition and analysis strategy enabled the annotation of a significant number (934) of LC−MS features. However, spectral information acquired by MS/MS often does not provide sufficient information to enable accurate characterization of structural details such as the double bond position or orientation, stereochemistry, or the position of the fatty acyl chain on the glycerol backbone.[71] Besides, potentially relevant metabolites (e.g., AA; sphingosines; or lipid peroxidation products such as IsoPs, isofuranes, and neuroprostanes) were not detected, most likely because of their low concentrations in the samples and the type of sample preprocessing. Further targeted lipid analysis of, e.g., PCs, LysoPC, ceramide, sphingomyelins, or lipid peroxides needs to be carried out to assess the abovementioned hypotheses.

CONCLUSIONS

The results showed changes in lipids associated with fatigue and clinically quiescent IBD. Significantly decreased levels of phosphatidylcholines, plasmanyls, sphingomyelins, lysophosphatidylcholines, phosphatidylethanolamines, phosphatidylinositols, phosphatidylserines, and eicosanoids were observed in patients with fatigue. Network and metabolic pathway analysis indicated a dysregulation of the arachidonic acid and glycerophospholipid metabolisms and the sphingolipid pathway. The protein−metabolite interaction network showed interactions between functionally related metabolites and proteins, displaying 40 hidden proteins in the network, including ABDH4, GLTP, and LCAT. Changes in the lipidomic profiles presented here should be further validated using a quantitative targeted approach in future studies involving larger sample sizes.

AUTHOR INFORMATION

Corresponding Authors

Guillermo Quintas − *Health and Biomedicine, LEITAT Technological Center, Barcelona 08028, Spain; Unidad Analítica, Health Research Institute Hospital La Fe, Valencia 46026, Spain;* orcid.org/0000-0002-4240-9846; Email: gquintas@leitat.org

Xavier Calvet − *Digestive Diseases Service, Hospital Universitari Parc Taulí, Institut d'Investigació i Innovació Parc Taulí I3PT and Departament de Medicina, Universitat Autònoma de Barcelona, Sabadell 08208, Spain; Centro de Investigación Biomédica en Red de Enfermedades Hepáticas y Digestivas CIBERehd, Instituto de Salud Carlos III, Madrid 28029, Spain;* Email: xcalvet@tauli.cat

Authors

Diana Horta − *Digestive Diseases Service, Hospital Universitari Parc Taulí, Institut d'Investigació i Innovació Parc Taulí I3PT and Departament de Medicina, Universitat Autònoma de Barcelona, Sabadell 08208, Spain*

Marta Moreno-Torres − *Unidad de Hepatología Experimental, Health Research Institute La Fe, Valencia 46026, Spain*

María José Ramírez-Lázaro − *Digestive Diseases Service, Hospital Universitari Parc Taulí, Institut d'Investigació i Innovació Parc Taulí I3PT, Universitat Autònoma de Barcelona, Sabadell 08208, Spain; Centro de Investigación Biomédica en Red de Enfermedades Hepáticas y Digestivas CIBERehd, Instituto de Salud Carlos III, Madrid 28029, Spain*

Sergio Lario − *Digestive Diseases Service, Hospital Universitari Parc Taulí, Institut d'Investigació i Innovació Parc Taulí I3PT, Universitat Autònoma de Barcelona, Sabadell 08208, Spain; Centro de Investigación Biomédica en Red de Enfermedades Hepáticas y Digestivas CIBERehd, Instituto de Salud Carlos III, Madrid 28029, Spain*

Julia Kuligowski − *Neonatal Research Group, Health Research Institute La Fe, Valencia 46026, Spain;* orcid.org/0000-0001-6979-2235

Juan Daniel Sanjuan-Herráez − *Health and Biomedicine, LEITAT Technological Center, Barcelona 08028, Spain*

Albert Villoria − *Digestive Diseases Service, Hospital Universitari Parc Taulí, Institut d'Investigació i Innovació Parc Taulí I3PT and Departament de Medicina, Universitat Autònoma de Barcelona, Sabadell 08208, Spain; Centro de Investigación Biomédica en Red de Enfermedades Hepáticas y Digestivas CIBERehd, Instituto de Salud Carlos III, Madrid 28029, Spain*

Complete contact information is available at: https://pubs.acs.org/10.1021/acs.jproteome.0c00462

Author Contributions

D.H. and M.M.-T. contributed equally to the study. D.H.: resources, writing−reviewing, and investigation; M.M.-T.:

https://dx.doi.org/10.1021/acs.jproteome.0c00462
J. Proteome Res. 2021, 20, 381−392

investigation and writing−reviewing; M.J.R.-L.: resources and investigation; S.L.: resources and investigation; J.K.: formal analysis; J.D.S.-H.: investigation; G.Q.: formal analysis, data curation, and writing−reviewing; A.V.: conceptualization and resources; and X.C.: conceptualization, methodology, supervision, and reviewing.

Notes

The authors declare no competing financial interest.

■ ACKNOWLEDGMENTS

M.M.-T. acknowledges support from the European Consortium EU-ToxRisk (EU Grant Agreement No. 681002). J.K. acknowledges the support received from Instituto de Salud Carlos III (Spain) with Grant Number CP16/00034.

■ REFERENCES

(1) Alatab, S.; Sepanlou, S. G.; Ikuta, K.; Vahedi, H.; Bisignano, C.; Safiri, S.; Sadeghi, A.; Nixon, M. R.; Abdoli, A.; Abolhassani, H.; Alipour, V.; Almadi, M. A. H.; Almasi-Hashiani, A.; Anushiravani, A.; Arabloo, J.; Atique, S.; Awasthi, A.; Badawi, A.; Baig, A. A. A.; Bhala, N.; Bijani, A.; Biondi, A.; Borzì, A. M.; Burke, K. E.; Carvalho, F.; Daryani, A.; Dubey, M.; Eftekhari, A.; Fernandes, E.; Fernandes, J. C.; Fischer, F.; Haj-Mirzaian, A.; Haj-Mirzaian, A.; Hasanzadeh, A.; Hashemian, M.; Hay, S. I.; Hoang, C. L.; Househ, M.; Ilesanmi, O. S.; Balalami, N. J.; James, S. L.; Kengne, A. P.; Malekzadeh, M. M.; Merat, S.; Meretoja, T. J.; Mestrovic, T.; Mirrakhimov, E. M.; Mirzaei, H.; Mohammad, K. A.; Mokdad, A. H.; Monasta, L.; Negoi, I.; Nguyen, T. H.; Nguyen, C. T.; Pourshams, A.; Poustchi, H.; Rabiee, M.; Rabiee, N.; Ramezanzadeh, K.; Rawaf, D. L.; Rawaf, S.; Rezaei, N.; Robinson, S. R.; Ronfani, L.; Saxena, S.; Sepehrimanesh, M.; Shaikh, M. A.; Sharafi, Z.; Sharif, M.; Siabani, S.; Sima, A. R.; Singh, J. A.; Soheili, A.; Sotoudehmanesh, R.; Suleria, H. A. R.; Tesfay, B. E.; Tran, B.; Tsoi, D.; Vacante, M.; Wondmieneh, A. B.; Zarghi, A.; Zhang, Z.-J.; Dirac, M.; Malekzadeh, R.; Naghavi, M. The Global, Regional, and National Burden of Inflammatory Bowel Disease in 195 Countries and Territories, 1990−2017: A Systematic Analysis for the Global Burden of Disease Study 2017. *Lancet Gastroenterol. Hepatol.* **2020**, *5*, 17−30.

(2) Ng, S. C.; Shi, H. Y.; Hamidi, N.; Underwood, F. E.; Tang, W.; Benchimol, E. I.; Panaccione, R.; Ghosh, S.; Wu, J. C. Y.; Chan, F. K. L.; Sung, J. J. Y.; Kaplan, G. G. Worldwide Incidence and Prevalence of Inflammatory Bowel Disease in the 21st Century: A Systematic Review of Population-Based Studies. *Lancet* **2017**, *390*, 2769−2778.

(3) Sairenji, T.; Collins, K. L.; Evans, D. V. An Update on Inflammatory Bowel Disease. *Prim. Care* **2017**, *44*, 673−692.

(4) Ungaro, R.; Mehandru, S.; Allen, P. B.; Peyrin-Biroulet, L.; Colombel, J.-F. Ulcerative Colitis. *Lancet* **2017**, *389*, 1756−1770.

(5) Borren, N. Z.; van der Woude, C. J.; Ananthakrishnan, A. N. Fatigue in IBD: Epidemiology, Pathophysiology and Management. *Nat. Rev. Gastroenterol. Hepatol.* **2019**, *16*, 247−259.

(6) Hindryckx, P.; Laukens, D.; D'Amico, F.; Danese, S. Unmet Needs in IBD: The Case of Fatigue. *Clin. Rev. Allergy Immunol.* **2018**, *55*, 368−378.

(7) Graff, L. A.; Clara, I.; Walker, J. R.; Lix, L.; Carr, R.; Miller, N.; Rogala, L.; Bernstein, C. N. Changes in Fatigue over 2 Years Are Associated with Activity of Inflammatory Bowel Disease and Psychological Factors. *Clin. Gastroenterol. Hepatol.* **2013**, *11*, 1140−1146.

(8) Guan, S.; Jia, B.; Chao, K.; Zhu, X.; Tang, J.; Li, M.; Wu, L.; Xing, L.; Liu, K.; Zhang, L.; Wang, X.; Gao, X.; Huang, M. UPLC−QTOF-MS-Based Plasma Lipidomic Profiling Reveals Biomarkers for Inflammatory Bowel Disease Diagnosis. *J. Proteome Res.* **2020**, *19*, 600−609.

(9) Fan, F.; Mundra, P. A.; Fang, L.; Galvin, A.; Moore, X. L.; Weir, J. M.; Wong, G.; White, D. A.; Chin-Dusting, J.; Sparrow, M. P.; Meikle, P. J.; Dart, A. M. Lipidomic Profiling in Inflammatory Bowel Disease: Comparison Between Ulcerative Colitis and Crohn's Disease. *Inflamm. Bowel Dis.* **2015**, *21*, 1511−1518.

(10) Villoria, A.; García, V.; Dosal, A.; Moreno, L.; Montserrat, A.; Figuerola, A.; Horta, D.; Calvet, X.; Ramírez-Lázaro, M. J. Fatigue in Out-Patients with Inflammatory Bowel Disease: Prevalence and Predictive Factors. *PLoS One* **2017**, *12*, No. e0181435.

(11) Harvey, R. F.; Bradshaw, J. M. A Simple Index of Crohn's-Disease Activity. *Lancet* **1980**, *315*, 514.

(12) Lewis, J. D.; Chuai, S.; Nessel, L.; Lichtenstein, G. R.; Aberra, F. N.; Ellenberg, J. H. Use of the Noninvasive Components of the Mayo Score to Assess Clinical Response in Ulcerative Colitis. *Inflamm. Bowel Dis.* **2008**, *14*, 1660−1666.

(13) Tinsley, A.; Macklin, E. A.; Korzenik, J. R.; Sands, B. E. Validation of the Functional Assessment of Chronic Illness Therapy-Fatigue (FACIT-F) in Patients with Inflammatory Bowel Disease. *Aliment. Pharmacol. Ther.* **2011**, *34*, 1328−1336.

(14) Martínez-Sena, T.; Luongo, G.; Sanjuan-Herráez, D.; Castell, J. V.; Vento, M.; Quintás, G.; Kuligowski, J. Monitoring of System Conditioning after Blank Injections in Untargeted UPLC-MS Metabolomic Analysis. *Sci. Rep.* **2019**, *9*, No. 9822.

(15) Kuligowski, J.; Sánchez-Illana, Á.; Sanjuán-Herráez, D.; Vento, M.; Quintás, G. Intra-Batch Effect Correction in Liquid Chromatography-Mass Spectrometry Using Quality Control Samples and Support Vector Regression (QC-SVRC). *Analyst* **2015**, *140*, 7810−7817.

(16) Sánchez-Illana, Á.; Pérez-Guaita, D.; Cuesta-García, D.; Sanjuan-Herráez, J. D.; Vento, M.; Ruiz-Cerdá, J. L.; Quintás, G.; Kuligowski, J. Model Selection for Within-Batch Effect Correction in UPLC-MS Metabolomics Using Quality Control - Support Vector Regression. *Anal. Chim. Acta* **2018**, *1026*, 62−68.

(17) Smith, C. A.; Want, E. J.; O'Maille, G.; Abagyan, R.; Siuzdak, G. XCMS: Processing Mass Spectrometry Data for Metabolite Profiling Using Nonlinear Peak Alignment, Matching, and Identification. *Anal. Chem.* **2006**, *78*, 779−787.

(18) Kuhl, C.; Tautenhahn, R.; Böttcher, C.; Larson, T. R.; Neumann, S. CAMERA: An Integrated Strategy for Compound Spectra Extraction and Annotation of LC/MS Data Sets. *Anal. Chem.* **2012**, *84*, 283−289.

(19) Hutchins, P. D.; Russell, J. D.; Coon, J. J. LipiDex: An Integrated Software Package for High-Confidence Lipid Identification. *Cell Syst.* **2018**, *6*, 621−625.

(20) Tsugawa, H.; Cajka, T.; Kind, T.; Ma, Y.; Higgins, B.; Ikeda, K.; Kanazawa, M.; VanderGheynst, J.; Fiehn, O.; Arita, M. MS-DIAL: Data-Independent MS/MS Deconvolution for Comprehensive Metabolome Analysis. *Nat. Methods* **2015**, *12*, 523−526.

(21) Kind, T.; Liu, K.-H.; Lee, D. Y.; DeFelice, B.; Meissen, J. K.; Fiehn, O. LipidBlast in Silico Tandem Mass Spectrometry Database for Lipid Identification. *Nat. Methods* **2013**, *10*, 755−758.

(22) Salek, R. M.; Steinbeck, C.; Viant, M. R.; Goodacre, R.; Dunn, W. B. The Role of Reporting Standards for Metabolite Annotation and Identification in Metabolomic Studies. *GigaScience* **2013**, *2*, No. 13.

(23) Ten-Doménech, I.; Martínez-Sena, T.; Moreno-Torres, M.; Sanjuan-Herráez, J. D.; Castell, J. V.; Parra-Llorca, A.; Vento, M.; Quintás, G.; Kuligowski, J. Comparing Targeted vs. Untargeted MS2 Data-Dependent Acquisition for Peak Annotation in LC-MS Metabolomics. *Metabolites* **2020**, *10*, No. 126.

(24) Stein, S. E.; Scott, D. R. Optimization and Testing of Mass Spectral Library Search Algorithms for Compound Identification. *J. Am. Soc. Mass Spectrom.* **1994**, *5*, 859−866.

(25) Smit, S.; van Breemen, M. J.; Hoefsloot, H. C. J.; Smilde, A. K.; Aerts, J. M. F. G.; de Koster, C. G. Assessing the Statistical Validity of Proteomics Based Biomarkers. *Anal. Chim. Acta* **2007**, *592*, 210−217.

(26) Westerhuis, J. A.; Hoefsloot, H. C. J.; Smit, S.; Vis, D. J.; Smilde, A. K.; van Velzen, E. J. J.; van Duijnhoven, J. P. M.; van Dorsten, F. A. Assessment of PLSDA Cross Validation. *Metabolomics* **2008**, *4*, 81−89.

(27) Pirhaji, L.; Milani, P.; Leidl, M.; Curran, T.; Avila-Pacheco, J.; Clish, C. B.; White, F. M.; Saghatelian, A.; Fraenkel, E. Revealing

Disease-Associated Pathways by Network Integration of Untargeted Metabolomics. *Nat. Methods* **2016**, *13*, 770−776.
(28) Chong, J.; Soufan, O.; Li, C.; Caraus, I.; Li, S.; Bourque, G.; Wishart, D. S.; Xia, J. MetaboAnalyst 4.0: Towards More Transparent and Integrative Metabolomics Analysis. *Nucleic Acids Res.* **2018**, *46*, W486−W494.
(29) Villoria, A.; García, V.; Dosal, A.; Moreno, L.; Montserrat, A.; Figuerola, A.; Horta, D.; Calvet, X.; Ramírez-Lázaro, M. J. Fatigue in Out-Patients with Inflammatory Bowel Disease: Prevalence and Predictive Factors. *PLoS One* **2017**, *12*, No. e0181435.
(30) Smilde, A. K.; Jansen, J. J.; Hoefsloot, H. C. J.; Lamers, R.-J. A. N.; van der Greef, J.; Timmerman, M. E. ANOVA-Simultaneous Component Analysis (ASCA): A New Tool for Analyzing Designed Metabolomics Data. *Bioinformatics* **2005**, *21*, 3043−3048.
(31) Rubingh, C. M.; Bijlsma, S.; Derks, E. P. P. A.; Bobeldijk, I.; Verheij, E. R.; Kochhar, S.; Smilde, A. K. Assessing the Performance of Statistical Validation Tools for Megavariate Metabolomics Data. *Metabolomics* **2006**, *2*, 53−61.
(32) Saccenti, E.; Hoefsloot, H. C. J.; Smilde, A. K.; Westerhuis, J. A.; Hendriks, M. M. W. B. Reflections on Univariate and Multivariate Analysis of Metabolomics Data. *Metabolomics* **2014**, *10*, 361−374.
(33) Bijlsma, S.; Bobeldijk, I.; Verheij, E. R.; Ramaker, R.; Kochhar, S.; Macdonald, I. A.; van Ommen, B.; Smilde, A. K. Large-Scale Human Metabolomics Studies: A Strategy for Data (Pre-) Processing and Validation. *Anal. Chem.* **2006**, *78*, 567−574.
(34) Clark, J. E.; Ng, W. F.; Watson, S.; Newton, J. L. The Aetiopathogenesis of Fatigue: Unpredictable, Complex and Persistent. *Br. Med. Bull.* **2016**, *117*, 139−148.
(35) Simons, K.; van Meer, G. Lipid Sorting in Epithelial Cells. *Biochemistry* **1988**, *27*, 6197−6202.
(36) Okada, Y.; Mugnai, G.; Bremer, E. G.; Hakomori, S. Glycosphingolipids in Detergent-Insoluble Substrate Attachment Matrix (DISAM) Prepared from Substrate Attachment Material (SAM). Their Possible Role in Regulating Cell Adhesion. *Exp. Cell Res.* **1984**, *155*, 448−456.
(37) Ogretmen, B.; Hannun, Y. A. Biologically Active Sphingolipids in Cancer Pathogenesis and Treatment. *Nat. Rev. Cancer* **2004**, *4*, 604−616.
(38) Mathias, S.; Peña, L. A.; Kolesnick, R. N. Signal Transduction of Stress via Ceramide. *Biochem. J.* **1998**, *335*, 465−480.
(39) Nikolova-Karakashian, M. N.; Reid, M. B. Sphingolipid Metabolism, Oxidant Signaling, and Contractile Function of Skeletal Muscle. *Antioxid. Redox Signal.* **2011**, *15*, 2501−2517.
(40) Maceyka, M.; Spiegel, S. Sphingolipid Metabolites in Inflammatory Disease. *Nature* **2014**, *510*, 58−67.
(41) Kobzik, L.; Reid, M. B.; Bredt, D. S.; Stamler, J. S. Nitric Oxide in Skeletal Muscle. *Nature* **1994**, *372*, 546−548.
(42) Reid, M. B.; Khawli, F. A.; Moody, M. R. Reactive Oxygen in Skeletal Muscle. III. Contractility of Unfatigued Muscle. *J. Appl. Physiol.* **1993**, *75*, 1081−1087.
(43) Reid, M. B.; Haack, K. E.; Franchek, K. M.; Valberg, P. A.; Kobzik, L.; West, M. S. Reactive Oxygen in Skeletal Muscle. I. Intracellular Oxidant Kinetics and Fatigue in Vitro. *J. Appl. Physiol.* **1992**, *73*, 1797−1804.
(44) Ferreira, L. F.; Smith, J. D.; Moylan, J. S.; Reid, M. B. Sphingomyelinase and Ceramide Increase Reactive Species and Depress Maximal Skeletal Muscle Force in Vitro. *FASEB J.* **2010**, *24*, No. 801.16.
(45) Bryan, P.-F.; Karla, C.; Alejandro, M.-T. E.; Elva, E.-P. S.; Gemma, F.; Luz, C. Sphingolipids as Mediators in the Crosstalk between Microbiota and Intestinal Cells: Implications for Inflammatory Bowel Disease. *Mediators Inflammation* **2016**, *2016*, No. 9890141.
(46) Kornhuber, J.; Rhein, C.; Müller, C. P.; Mühle, C. Secretory Sphingomyelinase in Health and Disease. *Biol. Chem.* **2015**, *396*, 707−736.
(47) Regulation of the Activity and Fatty Acid Specificity of Lecithin-Cholesterol Acyltransferase by Sphingomyelin and Its Metabolites, Ceramide and Ceramide Phosphate. https://europepmc.org/article/pmc/pmc1451158#free-full-text (accessed 20 May, 2020).
(48) Malakhova, M. L.; Malinina, L.; Pike, H. M.; Kanack, A. T.; Patel, D. J.; Brown, R. E. Point Mutational Analysis of the Liganding Site in Human Glycolipid Transfer Protein FUNCTIONALITY OF THE COMPLEX. *J. Biol. Chem.* **2005**, *280*, 26312−26320.
(49) Brown, R. E.; Mattjus, P. Glycolipid Transfer Proteins. *Biochim. Biophys. Acta* **2007**, *1771*, 746−760.
(50) Tuuf, J.; Mattjus, P. Membranes and Mammalian Glycolipid Transferring Proteins. *Chem. Phys. Lipids* **2014**, *178*, 27−37.
(51) Kjellberg, M. A.; Mattjus, P. Glycolipid Transfer Protein Expression Is Affected by Glycosphingolipid Synthesis. *PLoS One* **2013**, *8*, No. e70283.
(52) Kjellberg, M. A.; Backman, A. P. E.; Ohvo-Rekilä, H.; Mattjus, P. Alternation in the Glycolipid Transfer Protein Expression Causes Changes in the Cellular Lipidome. *PLoS One* **2014**, *9*, No. e97263.
(53) Tuuf, J.; Mattjus, P. Human Glycolipid Transfer Protein—Intracellular Localization and Effects on the Sphingolipid Synthesis. *Biochim. Biophys. Acta* **2007**, *1771*, 1353−1363.
(54) Sharma, K.; Schmitt, S.; Bergner, C. G.; Tyanova, S.; Kannaiyan, N.; Manrique-Hoyos, N.; Kongi, K.; Cantuti, L.; Hanisch, U.-K.; Philips, M.-A.; Rossner, M. J.; Mann, M.; Simons, M. Cell Type− and Brain Region−Resolved Mouse Brain Proteome. *Nat. Neurosci.* **2015**, *18*, 1819−1831.
(55) Yang, F.; Guan, Y.; Feng, X.; Rolfs, A.; Schlüter, H.; Luo, J. Proteomics of the Corpus Callosum to Identify Novel Factors Involved in Hypomyelinated Niemann-Pick Type C Disease Mice. *Mol. Brain* **2019**, *12*, 17.
(56) Barnden, L. R.; Crouch, B.; Kwiatek, R.; Burnet, R.; Fante, P. D. Evidence in Chronic Fatigue Syndrome for Severity-Dependent Upregulation of Prefrontal Myelination That Is Independent of Anxiety and Depression. *NMR Biomed.* **2015**, *28*, 404−413.
(57) van Meer, G.; Voelker, D. R.; Feigenson, G. W. Membrane Lipids: Where They Are and How They Behave. *Nat. Rev. Mol. Cell Biol.* **2008**, *9*, 112−124.
(58) Shevchenko, A.; Simons, K. Lipidomics: Coming to Grips with Lipid Diversity. *Nat. Rev. Mol. Cell Biol.* **2010**, *11*, 593−598.
(59) Germain, A.; Ruppert, D.; Levine, S. M.; Hanson, M. R. Metabolic Profiling of a Myalgic Encephalomyelitis/Chronic Fatigue Syndrome Discovery Cohort Reveals Disturbances in Fatty Acid and Lipid Metabolism. *Mol. Biosyst.* **2017**, *13*, 371−379.
(60) Nicolson, G. L.; Ash, M. E. Lipid Replacement Therapy: A Natural Medicine Approach to Replacing Damaged Lipids in Cellular Membranes and Organelles and Restoring Function. *Biochim. Biophys. Acta* **2014**, *1838*, 1657−1679.
(61) Stenson, W. F. The Universe of Arachidonic Acid Metabolites in Inflammatory Bowel Disease: Can We Tell the Good from the Bad? *Curr. Opin. Gastroenterol.* **2014**, *30*, 347−351.
(62) Hanna, V. S.; Hafez, E. A. A. Synopsis of Arachidonic Acid Metabolism: A Review. *J. Adv. Res.* **2018**, *11*, 23−32.
(63) Smith, G. I.; Atherton, P.; Reeds, D. N.; Mohammed, B. S.; Rankin, D.; Rennie, M. J.; Mittendorfer, B. Omega-3 Polyunsaturated Fatty Acids Augment the Muscle Protein Anabolic Response to Hyperinsulinaemia−Hyperaminoacidaemia in Healthy Young and Middle-Aged Men and Women. *Clin. Sci.* **2011**, *121*, 267−278.
(64) Cracowski, J.-L.; Bonaz, B.; Bessard, G.; Bessard, J.; Anglade, C.; Fournet, J. Increased Urinary F2-Isoprostanes in Patients with Crohn's Disease. *Am. J. Gastroenterol.* **2002**, *97*, 99−103.
(65) Brash, A. R. Arachidonic Acid as a Bioactive Molecule. *J. Clin. Invest.* **2001**, *107*, 1339−1345.
(66) Ahn, K.; McKinney, M. K.; Cravatt, B. F. Enzymatic Pathways That Regulate Endocannabinoid Signaling in the Nervous System. *Chem. Rev.* **2008**, *108*, 1687−1707.
(67) Liu, Z.; Wang, D.; Xue, Q.; Chen, J.; Li, Y.; Bai, X.; Chang, L. Determination of Fatty Acid Levels in Erythrocyte Membranes of Patients with Chronic Fatigue Syndrome. *Nutr. Neurosci.* **2003**, *6*, 389−392.

https://dx.doi.org/10.1021/acs.jproteome.0c00462
J. Proteome Res. 2021, 20, 381−392

(68) Lee, H.-C.; Simon, G. M.; Cravatt, B. F. ABHD4 Regulates Multiple Classes of N-Acyl Phospholipids in the Mammalian Central Nervous System. *Biochemistry* **2015**, *54*, 2539−2549.
(69) Maccarrone, M. Metabolism of the Endocannabinoid Anandamide: Open Questions after 25 Years. *Front. Mol. Neurosci.* **2017**, *10*, No. 166.
(70) Lord, C. C.; Thomas, G.; Brown, J. M. Mammalian Alpha Beta Hydrolase Domain (ABHD) Proteins: Lipid Metabolizing Enzymes at the Interface of Cell Signaling and Energy Metabolism. *Biochim. Biophys. Acta* **2013**, *1831*, 792−802.
(71) Koelmel, J. P.; Ulmer, C. Z.; Jones, C. M.; Yost, R. A.; Bowden, J. A. Common Cases of Improper Lipid Annotation Using High-Resolution Tandem Mass Spectrometry Data and Corresponding Limitations in Biological Interpretation. *Biochim. Biophys. Acta* **2017**, *1862*, 766−770.

https://dx.doi.org/10.1021/acs.jproteome.0c00462
J. Proteome Res. 2021, 20, 381−392